International Journal of New Chemistry, 2015, 2(2), 41-49
Published online January 2015 in http://www.ijnc.ir/. Original Article

Online ISSN 2383-188X

Open Access

A DFT study of the nuclear magnetic properties of fullerenes

KhadijehKalateh*, Sara Kheirollahpoor

Department of Chemistry, College of chemistry, Yadegar-e-Imam Khomeini(RAH) Shahre Rey Branch, Islamic Azad University,Tehran, Iran.

*Corresponding Author e-mail Address: kalateh@gmail.com

Received 30March 2015; Accepted 20 April 2015; Published 20 April 2015

Abstract

The stable configurations, electronic structure and magnetic properties of $B_{16}N_{16}$, B_8C_{24}, Al and P inserted $(BC_3)_8$ was studied by performing density functional theory (DFT) calculations of the NMR parameters. The results indicate that B_8C_{24} has semiconductivity property and be effectively modified by inserting groups due to the introduction of certain impurity states within the band gap of the pristine nanostructure, thereby reducing the band gaps. The band gap B_8C_{24} cage is reduced from 2.18 eV to 1.96 (for Al-inserted) and 1.76 eV (for P-inserted), respectively. The calculation of chemical shielding (CS) tensors shown that the B_8C_{24} inserted with Al and P atoms possess a C_{3v} local symmetry with special chemical shifts patterns. Theoretical analyses by molecular orbital under C_{3v} symmetry explain the impurity energy levels and chemical sheilding tensors.The present results are expected to open a way to change the electronic and magnetic properties of studied nanocages, which is helpful to design or develop novel nanodevices based on these structures.

Keywords: $B_{16}N_{16}$, B_8C_{24}, AlB_7C_{24}, $B_7C_{24}P$, Fullerene, Density Functional Theory

1. Introduction

The calculation of nuclear magnetic resonance (NMR) and nuclear quadrupole resonance (NQR) parameters using density functional theory (DFT) techniques have become a major and powerful tool in the investigation of molecular structure[1]. Many DFT studies on magnetic properties of nanostructures have been performed. The boron-11 and nitrogen-15 chemical shielding (CS) tensors were calculated to investigate the influence of carbon doping on the electronic structure properties of the (4,4) boron nitride nanotube[2]. The nuclear magnetic resonance (NMR) parameters of O-doped (10, 0) zigzag boron nitride nanotubes[1], the pristine and germanium-doped (10, 0) boron-nitride (BN) nanotube[3] and silicon–carbon (SiC) doped boron nitride nanotubes (BNNTs)[4] have been studied. The boron adsorption induced magnetism in zigzag boron nitride nanotubes[5], effect of tube radius on the electronic and magnetic properties of finite boron nitride zigzag nanotubes[6] and the transition metal ring functionalized tips of open-ended (5,5) boron nitride nanotube (BNNT)[7], and the influence of NH3-attaching on the NMR parameters in the zigzag BN nanotube[8] are the examples of changing propertis of nanotubes.

The geometrical structure, nuclear magnetic resonance (NMR) chemical shielding tensors, and chemical shifts of boron and nitrogen nuclei for five small boron nitride nanotubes (BNNTs, three zigzag and two armchair types) and boron nitride (BN) sheet[9], the properties and reactivity of Si-doped hexagonal boron nitride (*h*-BN) sheets[10], structure, electronic and magnetic properties of hexagonal boron nitride sheets doped by 5d transition metal atoms[11], the stable configurations, electronic, and magnetic properties of the functionalized boron nitride (BN) nanosheets by NHx (x = 0, 1, and 2) groups[12], Cu, Pd and Au metal adatom adsorption on different adsorption sites of graphene analog h-BN monolayer[13], structural, electronic, magnetic and optical properties of Fe_6 cluster adsorbed on the surface of a boron nitride sheet[14] have been studied.

Among other boron nitride nonostructures the properties of boron nitride (BN), boron phosphide (BP), aluminum nitride (AlN), and aluminum phosphide (AlP) nanocones[15], the electronic structure properties of boron nitride nanocone (BNNC) with 240° disclination[16], stable structural, electric and magnetic properties of manganese (Mn) atom adsorption on armchair hydrogen edge-terminated boron nitride nanoribbon (A-BNNRs)[17], a magnetic tunnel junction consisting of a boron nitride ribbon contacted by two semi-infinite electrodes composed of(3,0)ferromagnetic zig-zag grapheme ribbons[18], semiconductor–halfmetal–metal transition and magnetism of bilayer graphene nanoribbons/hexagonal boron nitride heterostructure[19], the structural, electronic and magnetic properties of Fe nanowire encapsulated in zigzag(n,0) BNNTs ($8 \leq n \leq 15$) [20], the energetic stability, electronic and magnetic properties of carbon-doped triangular boron nitride quantum dots (BNQDs)[21] has been investigated.

Structural and electronic properties of C_{24} and some of its derivatives for $C_{12}B_6N_6$, $B_6N_6C_{12}$ and $B_{12}N_{12}$[22], exploring ^{11}B and ^{15}N NMR parameters of C_{70-2x} $(BN)_x$ fullerenes (x = 3-25) in connection with local structures and curvature effects[23], the substitution satterns of boron−nitrogen (BN) fullerenes from C_{50} up to $C_{20}B_{15}N_{15}$ CBN ball[24],boron−nitrogen (BN) substitution of fullerenes from C_{60} to $C_{12}B_{24}N_{24}$ CBN Ball[25], the electronic and magnetic properties of the dumbbell-like structures of fullerene dimers with boron-nitride hexagonal bridges C108(BN)3n+6, and their carbon counterparts C120+6n, n = 1–10[26]have been studied to investigte the magnetic properties of boron nitride fullerenes.

In this work, theoretical calculations of NMR parameters are used to study the electronic structure and properties of some fullerenes consisting of $B_{16}N_{16}$, B_8C_{24}, AlB_7C_{24} and $B_7C_{24}P$. To achieve the purpose, we have performed density functional theory (DFT) calculations to optimize the geometrical structures and subsequently, we have calculated the NMR parameters for the optimized structures.

2. Computational details

All calculations have been performed using Gaussian03 software package[27].Full geometry optimizations are accomplished by means of Becke- three parameter density functional with Lee- Yang-Parr correlation functional (B3LYP)[28,29]with the 6-31G(d) basis sets[30]. The Chemcraft program was used for visual inspection of the normal modes and to propose an initial geometry of the investigated molecules. Using the ground state optimized geometry at the respective levels of theory. The NMR parameters have been calculated at the same level of computations based on the gauge-included atomic orbital (GIAO) approach [4/18]. It is noted that, in order to reproduce the NMR parameters, the calculated chemical shielding (CS) tensors in principal axes system (r_{33}> r_{22}> r_{11}) are converted to isotropic (CSI) and anisotropic (CSA) parameters using the following equations[31]:

$$CSI\ (ppm) = (\sigma_{11} + \sigma_{22} + \sigma_{33})/3 \quad (1)$$

$$CSA\ (ppm) = \sigma_{33} - (\sigma_{11} + \sigma_{22})/2 \quad (2)$$

The CSI parameter refers to the averaged electronicdensity at the atomic site whereas the CSA parameter indicates the difference between the distributionof the electronic densities perpendicular to the molecular plane (Z axis) and within the molecularplane (X–Y axes).

3. Results and discussion

3.1. Geometrical structures of $B_{16}N_{16}$, B_8C_{24}, AlB_7C_{24} and $B_7C_{24}P$ cages

The $B_{16}N_{16}$ cage is chosen to show the geometric structures of fullerene cages. The $B_{16}N_{16}$ cage is shown in Fig. 1(a). The geometric structures for $B_{16}N_{16}$, B_8C_{24} and AlB_7C_{24} cages are represented inFig. 1(b,c). The optimized structure for $B_7C_{24}P$ is similar to fig. 1c by P substitution instead of Al. When one heteroatom is insertedin the B_8C_{24}, the fullerene cage is reformed and the symmettry of structure is reduced significantly.

3.2. Electronic structure of $B_{16}N_{16}$, B_8C_{24}, AlB_7C_{24} and $B_7C_{24}P$ cages

Fig. 2 illustrates the molecular orbital diagrams the $B_{16}N_{16}$, B_8C_{24}, AlB_7C_{24} and $B_7C_{24}P$ cages. As shown in Fig. 2, the band gap of $B_{16}N_{16}$ appears at 6.37 eV which indicates insulating behavior for this cage. For

B_8C_{24}, AlB_7C_{24} and $B_7C_{24}P$ cages, the energy gaps exist at 2.18eV, 1.96 eVand 1.76 eV respectively which corresponding with semiconductivity property. The band gap was reduced by impurity in B_8C_{24} cage.

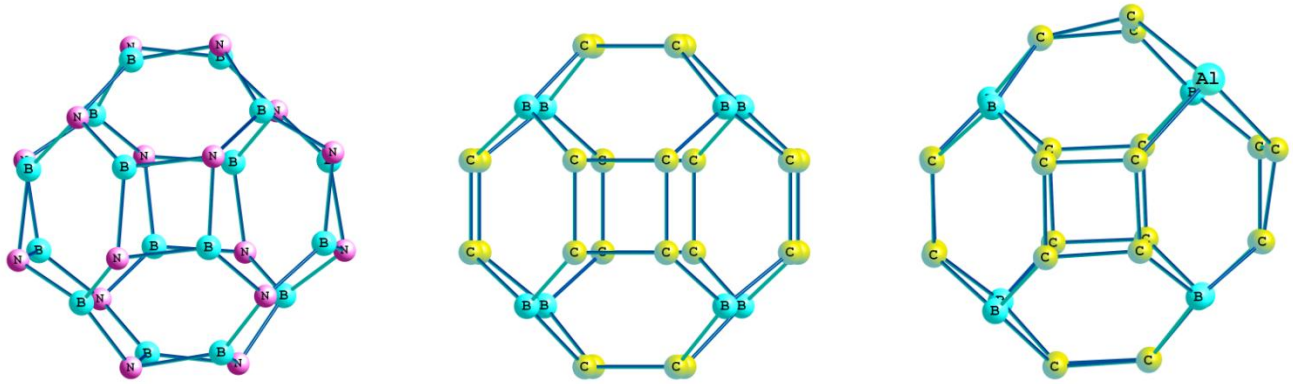

(a) $B_{16}N_{16}$ (b) B_8C_{24} (c) AlB_7C_{24}

D_{2d} O_h C_{3v}

Fig. 1. Optimized structures for $B_{16}N_{16}$, B_8C_{24}, AlB_7C_{24} fullerenes.

3.3. ^{15}N and ^{11}B nuclear magnetic properties calculations for $B_{16}N_{16}$, B_8C_{24}, AlB_7C_{24} and $B_7C_{24}P$ cages

The ^{15}N and $^{11}B\sigma_{iso}$ and σ_{aniso} values of the $B_{16}N_{16}$, B_8C_{24}, AlB_7C_{24} and $B_7C_{24}P$ cages are shown in Table 1-3.For the $B_{16}N_{16}$ cage fornitrogen atoms are equivalent with tetrahedron geometry and others are equivalent. Similar situation was observed for boron atoms as shown in Fig. 3a.and all the boron atoms are equivalent too, thereforethe ^{15}NNMR calculations of $B_{16}N_{16}$ cage show only two peaks at109 and 144 ppm and the ^{11}B NMR results two peaks at close to 79 and 77 ppm was observed for tetrahedral situation and others atom respectively. Similar patterns were observed for calculated σ_{aniso}values. The NMR chemical shift calculations of the B_8C_{24}cage show onepeak at -38.5 ppm for nitrogen atoms and one peak close to 81ppm for boron atoms which shows similar chemical environmetal for each atom type. For the $B_7C_{24}P$cages, there are three typepeaks, one peak at 668 ppm, 3 peaks around 536 ppm and 3 peaks around -0.6 ppm in ^{11}BNMR as shown in figure 1a. Boron atoms and phosphorous atom form a bicappedantiprismtiangular structure which P atom placed on the top of one caps. The largest chemical shift and chemical deshielding was observed for B7 which placed on the other top of antiprism while the lowest chemical shift and chemical sheilding was observed for B1, B2 and B3 atoms which locate on a triangle of antiprism near B7 atom. The chemical shift of B4, B5 and B6 atoms which form another triangle of antiprism near P atom are placed between two mentiond peaks. It is noticed that when the boron atoms is placed in the ring of including P atom the ^{13}B NMR chemical shift is increased due to the electron density around the carbon nucleus is deccreased and hence its shielding is decreased(B4, B5, B6). For B1, B2 and B3 that are placed on th opposite side of antiprism^{13}B NMR chemical shift are very low due to the electron density is increased. Similar pattern was observed for ^{13}C NMR too including triangles and hegzagons of carbon atoms with similar chemical shift and sheilding as depicted in figure 3b.There are six different positions of carbon atoms. The first position is triangles of carbons on the farthest of P atom (see values with pink color) at 482 ppm and the last one is observed for carbonsare positioned in eclipsed triangle of carbons far from P atom (see values with green color) at 963ppm.

Similar pattern was observed for chemical shift and sheilding of AlB_7C_{24}fulleren too but the turn of peaks is differenet as shown in the figure 3c and 3d.

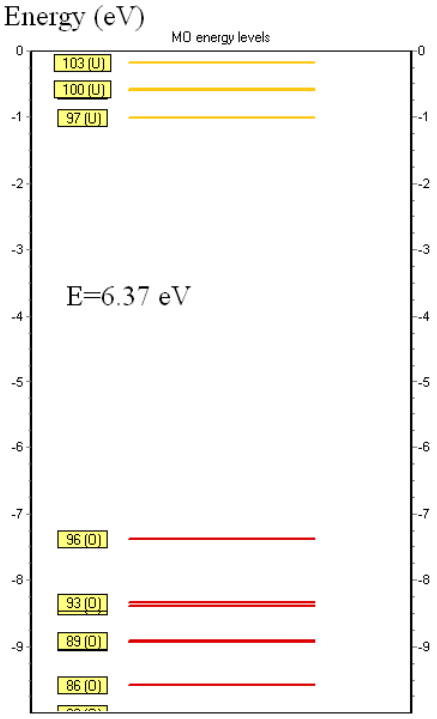

$B_{16}N_{16}$

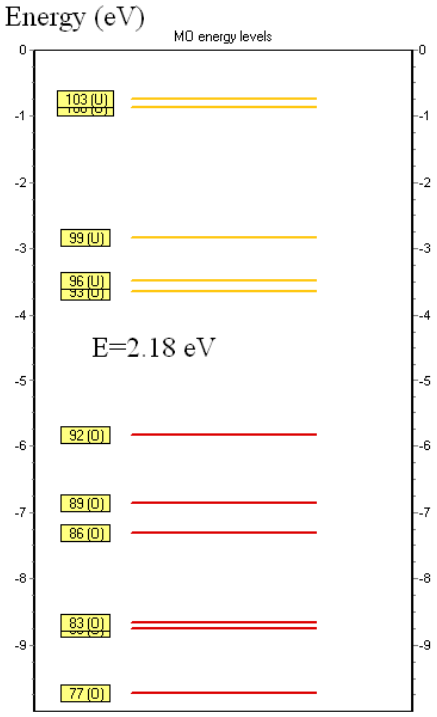

B_8C_{24}

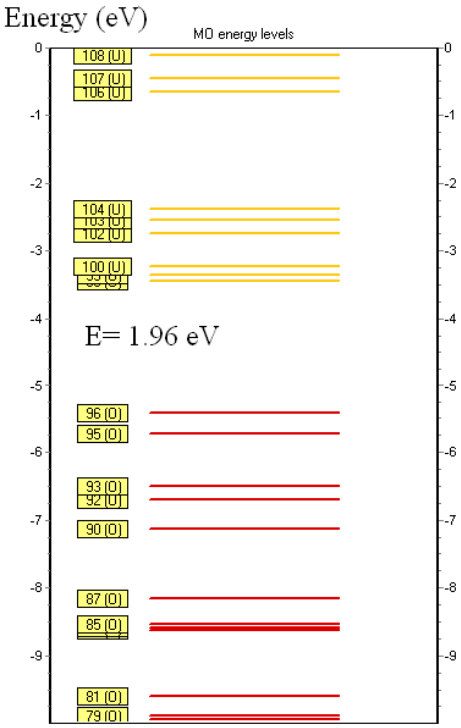

AlB_7C_{24}

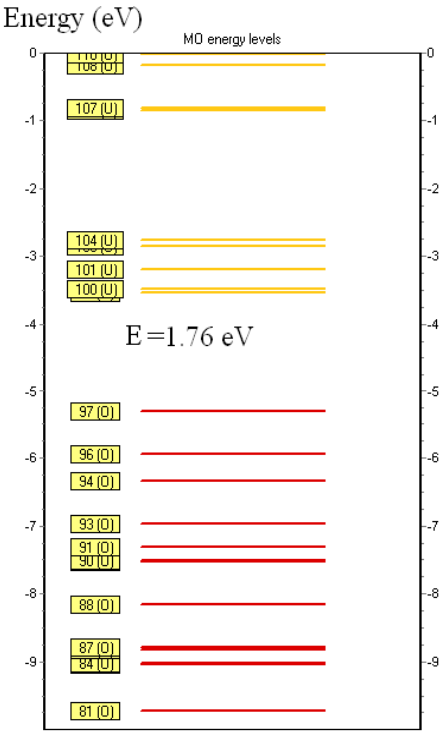

$B_7C_{24}P$

Fig. 2. Molecular orbital diagrams for $B_{16}N_{16}$, B_8C_{24}, AlB_7C_{24} and $B_7C_{24}P$ fullerenes.

Table 1. σ_{iso} and σ_{aniso} values for atoms combine $B_{16}N_{16}$

atom	σ_{iso}	σ_{aniso}
B1,B6,B11,B15	79.3263-79.4155	33.6339-33.8287
B2-B5,B7-B10,B12-B14,B16	76.8604-76.9765	35.0811-35.2169
N1-N3,N6-N10,N12-N14,N16	114.3532-114.6399	137.9885-138.6356
N4,N5,N11,N15	149.591-149.9005	166.4373-166.7085

Table 2. σ_{iso} and σ_{aniso} values for atoms combine B_8C_{24}

atom	σ_{iso}	σ_{aniso}
B1-B8	80.5689	64.8843
C1-C24	-38.4988	258.2589

Table 3. σ_{iso} and σ_{aniso} values for atoms combine $B_7C_{24}P$ and AlB_7C_{24}

	$B_7C_{24}P$		AlB_7C_{24}	
atom	σ_{iso}	σ_{aniso}	σ_{iso}	σ_{aniso}
B1	-0.6732	35.0139	72.6891	76.515
B2	-0.6732	35.0139	72.6891	76.515
B3	-0.5897	34.9214	72.7828	76.5802
B4	536.7519	1101.264	95.2145	53.7899
B5	535.5592	1096.922	95.2348	54.0453
B6	536.7519	1101.264	95.2145	53.7899
B7	667.8732	494.0223	80.7242	46.3079
P/Al	1003.888	499.2799	302.8784	142.0217
C1	567.4915	2383.855	-83.9824	263.9211
C2	570.5714	2390.788	-83.8771	263.6918
C3	570.5714	2390.788	-83.8771	263.6918
C4	-415.856	2740.086	-36.8683	247.9734
C5	-415.531	2729.552	-36.8702	247.8644
C6	-411.322	2735.612	-36.8822	248.0244
C7	-415.531	2729.552	-36.8702	247.8644
C8	-415.856	2740.086	-26.8683	247.9734
C9	-411.322	2735.612	-36.8822	248.0244
C10	962.997	1934.633	-36.8647	254.2256
C11	962.997	1934.634	-36.8647	254.2256
C12	960.9209	1926.41	-36.8589	254.132
C13	263.0024	977.0437	-45.0508	256.4115
C14	97.7807	4306.408	-9.6818	166.9913
C15	262.5004	975.4165	-45.0104	256.2553
C16	97.3118	4295.412	-9.7054	166.9944
C17	97.3118	4295.412	-9.7054	166.9944
C18	262.5004	975.4165	-45.0104	256.2553
C19	263.0024	977.0437	-45.0508	256.4115

C20	261.8705	974.7166	-45.0251	256.2911
C21	-481.552	869.1704	-28.6126	250.057
C22	261.8705	974.7166	-45.0251	256.2911
C23	-481.968	869.345	-28.6348	250.1572
C24	-481.968	869.345	-28.6348	250.1572

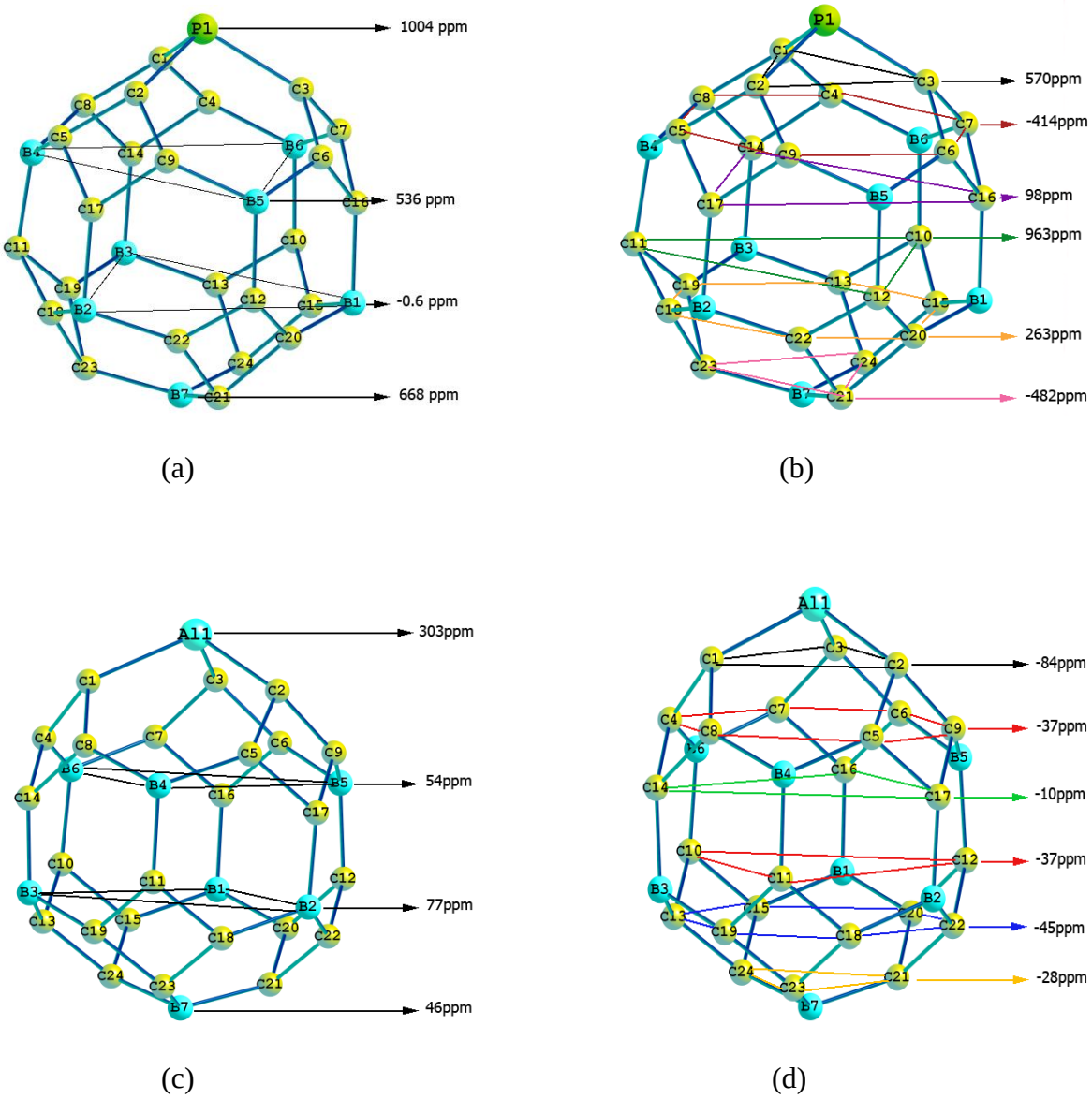

(a) (b)

(c) (d)

Fig 3. Calculated σ_{iso} of $B_7C_{24}P$ (a,b) and AlB_7C_{24} (c,d)

4. Conclusion

The electronic structure and magnetic properties of $B_{16}N_{16}$, B_8C_{24}, AlB_7C_{24} and $B_7C_{24}P$ was studied by performing density functional theory (DFT) calculations. The calculations of NMR parameteres show two type boron and nitrogen atoms in $B_{16}N_{16}$ while all of boron and carbon atoms are equivalent in B_8C_{24}. The AlB_7C_{24} and $B_7C_{24}P$ C_{3v} local symmetry have three type boron and six type carbon atoms with different chemical shifts. The calculations indicate $B_{16}N_{16}$ with 6.37 eV band gap is insulator but the other fullerenes

are semiconductor and the band gap reduced by impurity inserting so the band gap of Al-inserted cage is 1.96 eV and the band gap of P-inserted cage is 1.76 eV in comparison of pristine fullerene with 2.18 eV band gap. As the result the spectral properties can used to pridict the geometry and electronic properties can used to predict sensing conductivity behavior in studied structures.

Acknowledgment

We are appreciating and thanking Islamic Azad University of Yeager-e-Imam Khomeini (RAH) Shahre Rey.

References

1. Seif, A., Boshra, A., Journal of Molecular Structure: THEOCHEM 2009, 895 (1–3), 96-99.

2. Mirzaei, M., Physica E: Low-dimensional Systems and Nanostructures 2009, 41 (5), 883-885.

3. Wang, R., Zhang, D., Liu, C., Computational Materials Science 2014, 82, 361-366.

4. Mirzaei, M., Physica E: Low-dimensional Systems and Nanostructures 2010, 42 (7), 1954-1957.

5. Li, L. L., Yang, S. Q., Yang, X. J., Xu, X. W., Tang, C. C., Journal of Molecular Structure 2012, 1020, 183-187.

6. Zahedi, E., Seif, A., Physica E: Low-dimensional Systems and Nanostructures 2011, 44 (1), 179-185.

7. Zhao, J.-x., Ding, Y.-h., Journal of Physics and Chemistry of Solids 2009, 70 (6), 1030-1033.

8. Zahedi, E., Bodaghi, A., Seif, A., Boshra, A., Superlattices and Microstructures 2011, 49 (2), 169-175.

9. Bagheri, Z.; Abolhassani, M. R.; Hadipour, N. L., Physica E: Low-dimensional Systems and Nanostructures 2008, 41 (1), 124-129.

10. Liu, Y.-j.; Gao, B.; Xu, D.; Wang, H.-m.; Zhao, J.-x., Physics Letters A 2014, 378 (40), 2989-2994.

11. Zhang, Z.; Geng, Z.; Cai, D.; Pan, T.; Chen, Y.; Dong, L.; Zhou, T., Physica E: Low-dimensional Systems and Nanostructures 2015, 65, 24-29.

12. Tang, S.-l., Liu, Y.-j., Wang, H.-x., Zhao, J.-x., Cai, Q.-h., Wang, X.-z., Diamond and Related Materials 2014, 44, 54-61.

13. Sen, D., Thapa, R., Bhattacharjee, K., Chattopadhyay, K. K., Computational Materials Science 2012, 51 (1), 165-171.

14. Moradian, R., Shahrokhi, M., Sadat Charganeh, S., Moradian, S., Physica E: Low-dimensional Systems and Nanostructures 2012, 46, 182-188.

15. Mirzaei, M., Yousefi, M., Meskinfam, M., Superlattices and Microstructures 2012, 51 (6), 809-813.

16. Nouri, A., Mirzaei, M., Journal of Molecular Structure: THEOCHEM 2009, 913 (1–3), 207-209.

17. Abdullahi, Y. Z., Rahman, M. M., Shuaibu, A., Abubakar, S., Zainuddin, H., Muhida, R., Setiyanto, H., Physica B: Condensed Matter 2014, 447, 65-69.

18. Padilha, J. E., Pontes, R. B., da Silva, A. J. R., Fazzio, A., Solid State Communications 2013, 173, 24-29.

19. Ilyasov, V. V., Meshi, B. C., Nguyen, V. C., Ershov, I. V., Nguyen, D. C., Solid State Communications 2014, 199, 1-10.

20. Wang, S.-F., Zhang, J.-M., Xu, K.-W., Physica B: Condensed Matter 2010, 405 (4), 1035-1039.

21. Xi, Y., Zhao, X., Wang, A., Wang, X., Bu, H., Zhao, M., Physica E: Low-dimensional Systems and Nanostructures 2013, 49, 52-60.

22. Anafche, M., Naderi, F., 2012.

23. Anafcheh, M., Ghafouri, R., Monatsh Chem 2014, 145 (3), 411-419.

24. Xu, X., Shang, Z., Wang, G., Li, R., Cai, Z., Zhao, X., The Journal of Physical Chemistry A 2005, 109 (16), 3754-3761.

25. Pattanayak, J., Kar, T., Scheiner, S., The Journal of Physical Chemistry A 2002, 106 (12), 2970-2978.

26. Anafcheh, M., Ghafouri, R., Computational and Theoretical Chemistry 2012, 1000, 85-91.

27. Frisch, M. J., Trucks, G. W., Schlegel, H. B., Scuseria, G. E., Robb, M. A., Cheeseman, J. R., Montgomery, J. A., Vreven, T., Kudin, K. N., Burant, J. C., Millam, J. M., Iyengar, S. S., Tomasi, J., Barone, V., Mennucci, B., Cossi, M., Scalmani, G., Rega, N., Petersson, G. A., Nakatsuji, H., Hada, M., Ehara, M., Toyota, K., Fukuda, R., Hasegawa, J., Ishida, M., Nakajima, T., Honda, Y., Kitao, O., Nakai, H., Klene, M., Li, X., Knox, J. E., Hratchian, H. P., Cross, J. B., Bakken, V., Adamo, C., Jaramillo, J., Gomperts, R., Stratmann, R. E., Yazyev, O., Austin, A. J., Cammi, R., Pomelli, C., Ochterski, J. W., Ayala, P. Y., Morokuma, K., Voth, G. A., Salvador, P., Dannenberg, J. J., Zakrzewski, V. G., Dapprich, S., Daniels, A. D., Strain, M. C., Farkas, O., Malick, D. K., Rabuck, A. D., Raghavachari, K., Foresman, J. B., Ortiz, J. V., Cui, Q., Baboul, A. G., Clifford, S., Cioslowski, J., Stefanov, B. B., Liu, G., Liashenko, A., Piskorz, P., Komaromi, I., Martin, R. L., Fox, D. J., Keith, T., Laham, A., Peng, C. Y., Nanayakkara, A., Challacombe, M., Gill, P. M. W., Johnson, B., Chen, W., Wong, M. W., Gonzalez, C., Pople, J. A., ed., Vol., 2003.

28. Becke, A. D., The Journal of Chemical Physics 1993, 98 (7), 5648-5652.

29. Lee, C., Yang, W., Parr, R. G., Physical Review B 1988, 37 (2), 785-789.

30. Binkley, J. S., Pople, J. A., Hehre, W. J., Journal of the American Chemical Society 1980, 102 (3), 939-947.

31. Drago, R.S., Physical Methods for Chemists, Saunders, New York, 1992